Calculating Two-Dimensional Fourier Transforms I. Performance II. Normalization III. Graphics

Maricor Soriano, Grace Gerella and Caesar Saloma
Instrumentation Physics Laboratory
National Institute of Physics, College of Science
University of the Philippines
Diliman, Quezon City

ABSTRACT

A scientific software for calculating the Fourier transforms of two-dimensional functions is presented in detail. It performs forward and inverse calculations, normalization and three-dimensional graphics display (modulus versus xy space). Implementation of software is achieved in a minimum environment of an IBM PC-XT microcomputer with a mathematical co-processor. Calculation of the transfer function of a grating spectrometer and high-pass image filtering are used as performance benchmarks. Considerations regarding proper normalization of result and its effective display in 3-D graphics (Floating Horizon algorithm) to minimize the number of hidden lines are also discussed.

INTRODUCTION

Analysis and processing of signals can be done both in their real (space/time) or frequency (spectrum) representation. Capability to examine the various properties in either domain is crucial in instrument design and signal/image processing. For instance,

filter design and bandwidth determination are done easily in the frequency domain of a given signal. While most signals are usually measured in the real domain, there are instances wherein their corresponding spectra are of primary interest. Such are in Fourier transform spectroscopy, image reconstruction using deconvolution techniques and data compression. The ability to transform efficiently and quickly any signal (real domain) into its equivalent spectral representation (frequency domain) and vice versa, depends on the availability of a reliable computer software that requires less complicated hardware without sacrificing speed, resolution and bandwidth.

In a linear-shift invariant (LSI) measuring apparatus, the measured signal o(**x**) results from the convolution of the original (input) signal i(**x**) with the point-spread function h(**x**), i.e. o(**x**) = i(**x**) * * h(**x**) where **x** is an N-dimensional real variable. Since h(**x**) will not have the properties of a Dirac delta function due to bandwidth limitation of real physical systems, the measured signal o(**x**) is never a one-to-one mapping from the input space to output space. Since the quantity of interest is i(x), a procedure to restore or recover it from o(**x**) must be implemented. This recovery procedure is easier done in the frequency domain because of the equivalent relation O(f) = I(**f**)H(f) where O(**f**),I(**f**) and H(**f**) are the Fourier transforms of o(**x**), i(**x**) and h(**x**), respectively and f is N-dimensional frequency variable. By calculating O(**f**)/H(**f**) and performing an inverse Fourier transform on the result, the input function i(**x**) is determined. Thus, knowledge of the transfer function H(**f**), brings about both maximum recovery of available information and complete understanding of the measuring instrument itself.

In this paper, we present a scientific software that was developed at the National Institute of Physics. It was written as a utility program in instrumentation design and requires a minimum hardware of an IBM PC-XT compatible with an 8087 math co- processor.

The paper is organized as follows: II. Fourier Transformation of Two-Dimensional Discrete Signals (Cooley-Tukey Algorithm); III. A. Implementation: Point Spread Function of a Spectrometer, B. A Scene Under High-Pass Filtering, IV. Normalization; V. Graphics Display With Minimum Hidden Lines.

FOURIER TRANSFORMATION OF TWO-DIMENSIONAL DISCRETE SIGNALS

The discrete Fourier transform in one-dimension is given by

$$X\left(\frac{m}{MD_x}\right) = A\sum_{k=0}^{M} x(kD_x)e^{-\frac{j2\pi mk}{M}} \qquad (1)$$

where A is a constant, M is the number of data points, D_x is the sampling interval and (k,m) are the indices of the discrete input data and the corresponding Fourier coefficients, respectively. For the two-dimensional function $z(kD_x,lD_y)$ the corresponding discrete Fourier transform $Z(m/MD_x,n/ND_y)$ is given by

$$Z\left(\frac{m}{MD_x},\frac{n}{ND_y}\right) = \sum_{l=0}^{M-1}\sum_{k=0}^{N-1} z(kD_x,lD_y)e^{-\frac{j2\pi mk}{N}}e^{-\frac{j2\pi ml}{M}} \qquad (2)$$

Implementation of Eqn. (2) involves the sequential calculation of one-dimensional Fourier coefficients. The number of operations required in determining the coefficients by direct calculation of Eqn. (1) obeys a square law relation with the number of data points M.

Cooley and Tukey[1] developed a more efficient (less number of operations and memory space for the same number of data points) algorithm for calculating one-dimensional Fourier coefficients for the special case when $M = 2^y$ i.e. the number of data points is expressible in powers of 2. Using the following notations:

$$X(m) = \sum_{k=0}^{M-1} x(k)W^{mk} \qquad (3)$$

where

$$W = e^{-\frac{j2\pi}{M}}$$

Equation (1) readily assumes the form of a matrix equation with the W^{mk} factorable into y separate square matrices containing only 1's, 0's, and W^{mk}'s. To carry out the factorization, a bit-

reversal of the ordering of the discrete Fourier coefficients is needed. The bit-reverse of a number is calculated by taking its binary equivalent, reversing the order of its bits and converting it back to its numeral equivalent.

Using $W^{mk} = W^P$ with $W^P = W^{P+M/2}$, then

$$x_1(k) = x_{l-1}(k) + W^P x_{l-1}\left(k + \frac{M}{2^l}\right) \quad (4)$$

and

$$x_1\left(k + \frac{M}{2^l}\right) = x_{l-1}(k) - W^P x_{l-1}\left(k + \frac{M}{2^l}\right) \quad (5)$$

Equations (4) and (5) constitute a dual-node pair and are the key to the efficiency of the FFT algorithm. Except for the sign, the values in the dual-node pair are periodic in $k + M/2^1$. Thus calculation involving dual node pairs effectively cuts the number of operations by half.

Direct calculations of the Fourier coefficients take cN^2 seconds (c is a proportionality factor) to accomplish. In the one-dimensional Cooley-Tukey algorithm, the number of necessary multiplications is reduced from N^2 to $M\gamma/2$. In two dimensions with $M = N$, the computation time for direct calculations would be proportional to $2M^3$ while the Cooley-Tukey algorithm takes only $M\gamma^2$.

We transcripted the Cooley-Tukey algorithm using Turbo-Pascal Version 5. The computer we used for calculations was a 10MHz IBM XT V6.0 equipped with an 8087 Math co-processor.

IMPLEMENTATION

Two specific cases are taken to show the performance of our software.

A. The point-spread function of a spectrometer employing phase-grating as aperture

The spectrometer functions as a coherent imaging system in which the entrance slit is imaged into the exit plane at unit magnification. The aperture of the optical system is assumed by the functional characteristics of the phase grating. Due to the finiteness of the aperture, the operational resolution (slit width,

aberrations and focal lengths are taken into consideration) of the spectrometer can not attain the resolution set by the grating relation, $\Delta\lambda = \lambda_{blaze}/pA$ where p is the diffraction order and A is the total number of equally-spaced lines in the grating.

The operational resolution is determined by calculating the point-spread function (PSF) of the spectrometer system. The PSF is calculated from the Fourier transform of the pupil function using the relation[2]; $h(x,y) = (1/f\ \lambda_{blaze})^2\ \mathbf{F}_{2D}$[grating function g(x,y)] where f is the focal length of the focusing mirror. The phase grating function (infinitely long in the x-direction) is given by[3]:

$$g(x,y) = \cos\left(\frac{\phi}{2}\right) + \frac{4i}{\pi}\sin\left(\frac{\phi}{2}\right)\sum_{q=0}^{Q}\frac{\sin(2q+1)\pi\frac{x}{a}}{2q+1} \quad (6)$$

where $\varphi = 4\pi e/\lambda_{blaze}$, e = line depth and a = width of line. Figure 5a shows the square (intesity distribution) of the Fourier transform of Eqn. (5) (line density = 1800 lines/mm or a = 0.56 μm, N = 1024, sampling distance a/4, λ_{blaze} = 550 nm, Q = 200). Since the slit function is essentially one-dimensional, the computation of the PSF simplifies into a one-dimensional exercise. Figure 5a illustrates the multiple images arising from the different diffraction orders with the zeroth-order image 60 times more intense than the first-order image. This is expected as there is no blaze angle introduced in the calculation.

Figure 5b shows a magnified view of the more useful first diffraction order. It is seen that the effective resolution of an infinitely narrow line in the entrance plane is limited due to the existence of a finite linewidth and side lobes. These are composite effects due to the finite value of Q in Eqn. (1) and the finite extent of the grating. Although gratings have been used as a dispersion optical element for years, its value as a light scatterer continues to attract researchers[4].

B. High-Pass Filtering of A Two-Dimensional Signal

High-pass filtering is a useful technique in locating the edges in the scene by suppressing irradiance of areas that are uniformly distributed [5]. Edges represent abrupt changes in the pixel-to-pixel

irradiance across the image field. Although high- emphasis filtering is also achieved through the application of a Laplacian operator on the data set (real domain), the same results can be obtained easily by deconvolution in the frequency domain.

Figure 2a shows radiance profile of the original scene (two keys, 128 x 128 pixels) taken by a CCD camera (Tektronix 1001 Video Camera, 490 x 384 pixels) and digitized using a Black/White frame grabber (Tektronix DCS01, 512 x 512 pixels). Its corresponding two-dimension spatial spectrum is presented in Figure 2b. Figure 2c shows the radiance profile of the reconstructed image done by performing an inverse Fourier transformation on the spectrum high-pass filtered with a step function ($f_{3\ dB}$ = 0.50 1/pixel size of CCD camera). Figure 2d shows a tonal profile of the filtered image.

NORMALIZATION

A waveform is normalized by assigning to its maximum amplitude the value of unity. The proportionality factor A in Eqn. (1) is introduced to make the analytic and discrete FT equivalent, i.e.

$$x(f) \cong AX\left(\frac{m}{MD_x}\right) \qquad (7)$$

Well-known references [6-8] have assigned different values for this constant: A = 1/M [*Brigham*] ; A = 1/sqrt(2p) [*Bracewell*] ; A = D_x [*W. Press et al*]. We have observed that different waveforms require different values of the normalization constant. Figure 3 illustrates the normalization constants for some waveforms (a: sinc, b: $sinc^2$ i, c: cos d: plane, and e: sombrero) commonly encountered in image/signal processing.

GRAPHICS

The ultimate goal in the graphics display of a three-dimensional field with two independent variables is always the full visualization of all its points. This is an impossible task to achieve

with the usual coordinate systems due to the depth of field requirement. The practical goal, therefore, is to find the coordinate orientation that displays the field with a sense of volume with the least number of points (or lines) hidden.

The plot of the set of one-dimensional Fourier coefficients is symmetrical with respect to M/2 with the points from M/2 to M-1 comprising the negative half of the graph.

In two dimensions, the negative and the positive half of the output are interchanged in both dimensions. Thus the output is quartered and appears at the corners. Besides bit-reversing, a procedure to interchange the quarters of the output must be included in any software implementation of the two-dimensional FFT.

The graphics output of the program is a three-dimensional surface in which the two space coordinates (x,y) are oriented, respectively, by angles α and β from the horizontal. The modulus of the Fourier coefficients constitute the vertical axis. Three-dimensional surface graphics draw the surface by planes. From the plane, which is apparently closest to the observer to the farthest plane, curves of the surface in that plane are drawn by drawing lines between sample points. To preserve the depth as well as to prevent confusion, curves hidden by other curves of closer planes must not be plotted. To accomplish this, a part of the Floating Horizon Algorithm was used[8].

This part of the floating horizon algorithm works as follows: if, at any given horizontal position, the vertical value of the curve in the current plane is larger than the maximum vertical value, or smaller than the minimum vertical value for any previous curve at that horizontal position, then the curve is visible; otherwise, it is hidden. In order to check whether a vertical value is smaller or larger than all previous values, the largest vertical value -- the upper horizon -- and the smallest vertical value -- the lower horizon -- are stored in arrays with horizontal position indices.

The graphics routine is implemented by two nested loops of two steps. The outer loop runs planes from the plane apparently closest to the observer to the farthest plane. The inner loop runs the horizontal positions from lowest to highest. Inside the inner loop are two steps: the first step computes the screen horizontal and vertical position of the current curve, from the modulus and the space coordinates via simple trigonometric conversion of the three dimensional data to the flat screen and simple screen scaling; the second step does a floating horizon test on the current screen value of the curve and plots the appropriate segments. An

unscrambling procedure first fixes the order of the bit-reversed output and then interchanges the halves in x and y.

In general, the discrete Fourier coefficient is a complex quantity. What we plot as output is the modulus of the real and imaginary FT. Figure 4a-c illustrates how the visual perception a one-dimensional $sinc^2$ function varies with the values of (α,β): A. $\alpha = 45°, \beta = 0$; B. $\alpha = 0°, \beta = 45$; C. $\alpha = 30°, \beta = 15°$; and D. $\alpha = 20°, \beta = 20°$. Note that the choice of optimal information display depends on the symmetry of the function.

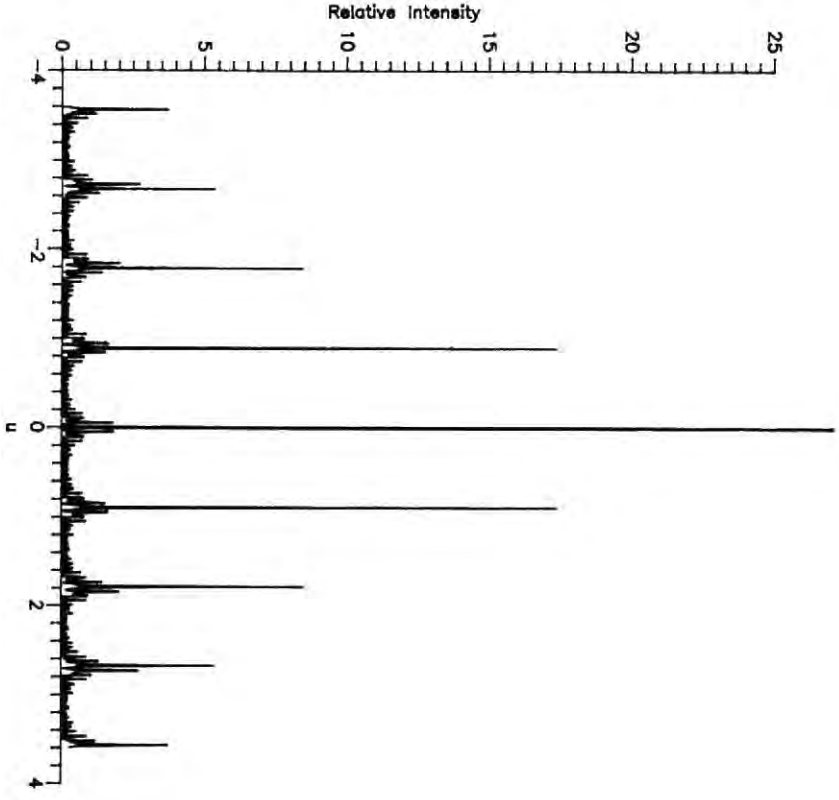

Figure 1a. Multiple images of a Dirac δ (infinitely narrow slit) when the aperture is a phase grating (line density = 1800 lines/mm, N = 1024 points, sampling distance = 0.14μm, period = 0.56 μm, λ=550nm, Q = 200)

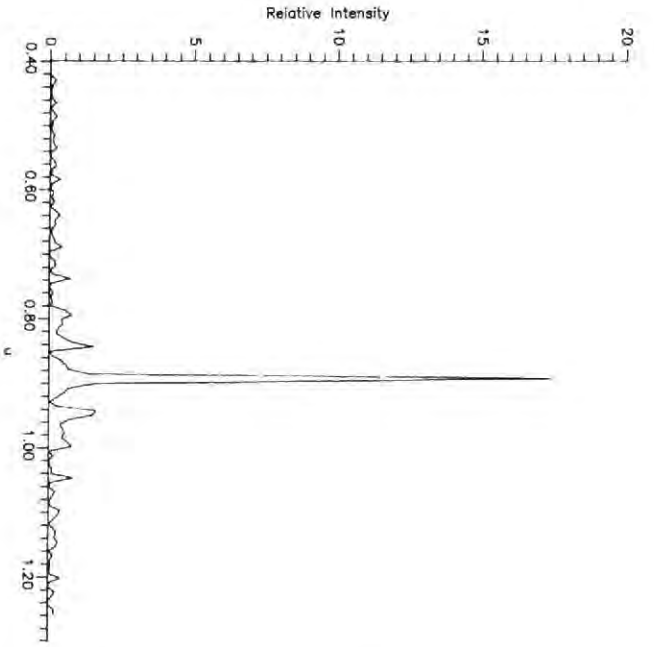

Figure 1b. Magnified version of the first order image

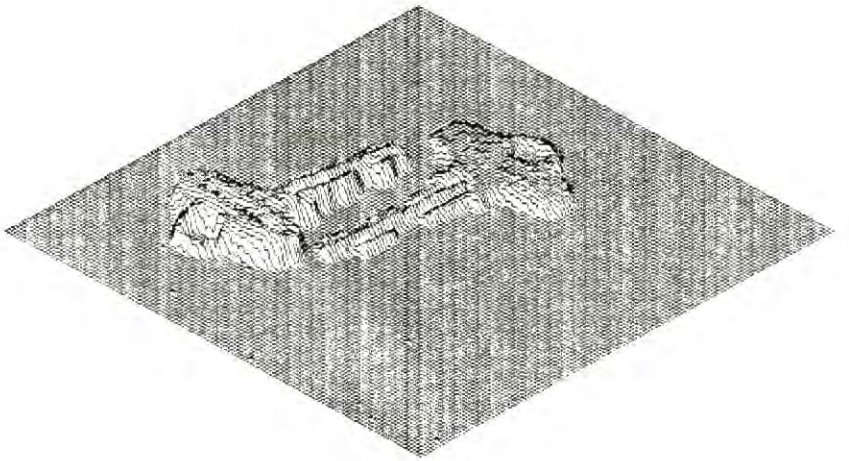

Figure 2a. Intensity profile of original image (two keys)

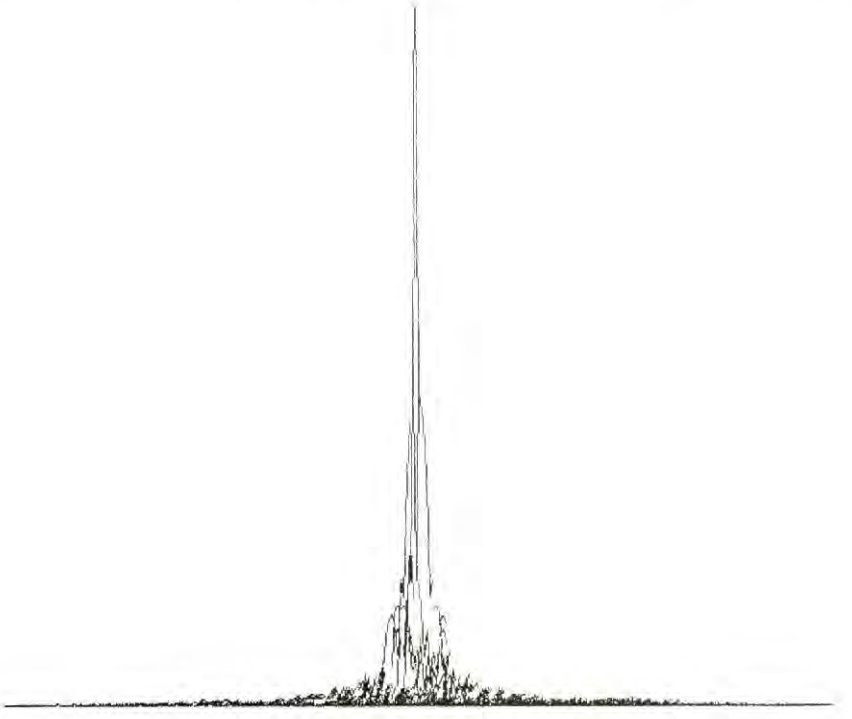

Figure 2b. Two-dimensional Fourier transform of image

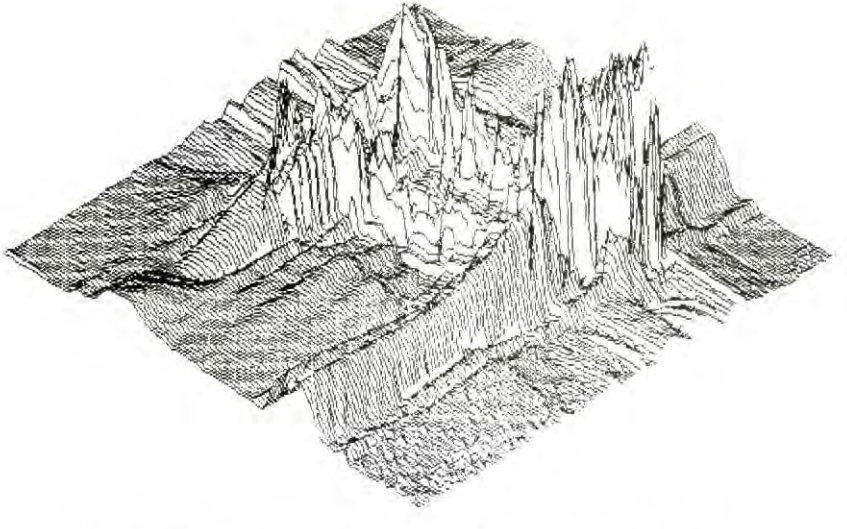

Figure 2c. Intensity profile of high-pass filtered image

ii. filtered image

i. original image

Figure 2d. Tonal version of original and filtered image

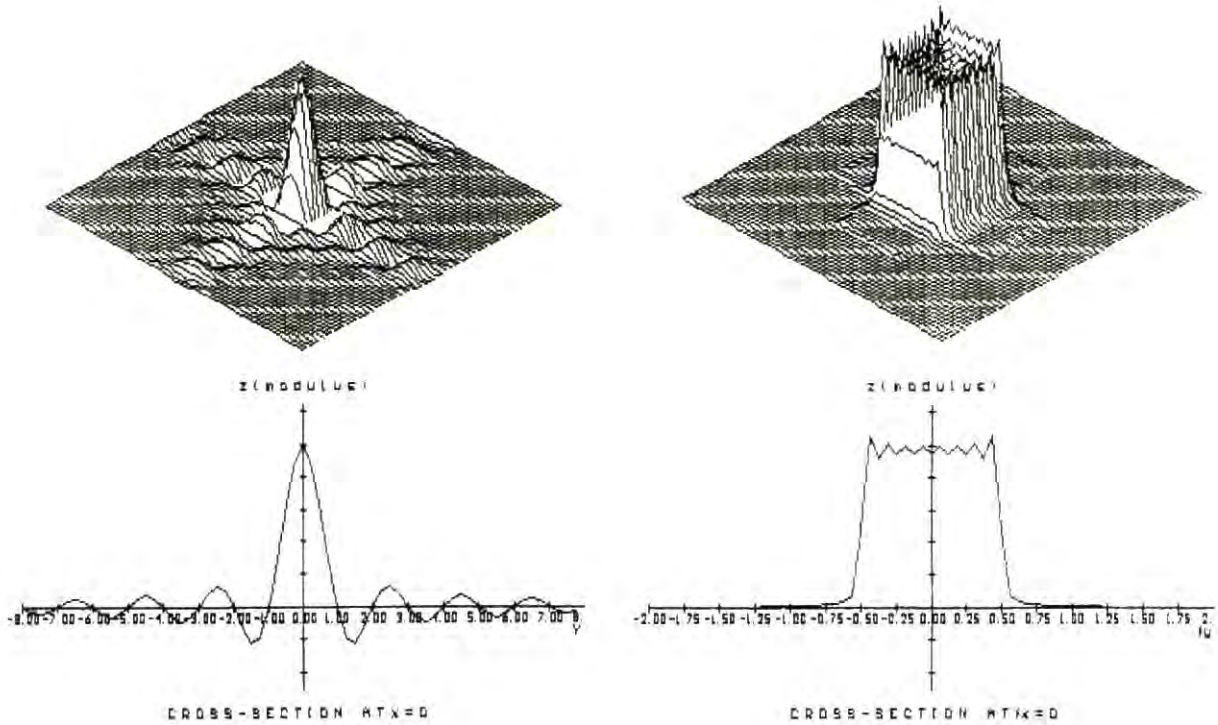

Figure 3. Normalization constants for various waveforms: a) sinc, A = DxDy. Left: Input Function, right: FT of Input Function, top: 3-d graph, bottom: 2-d view at x + 0

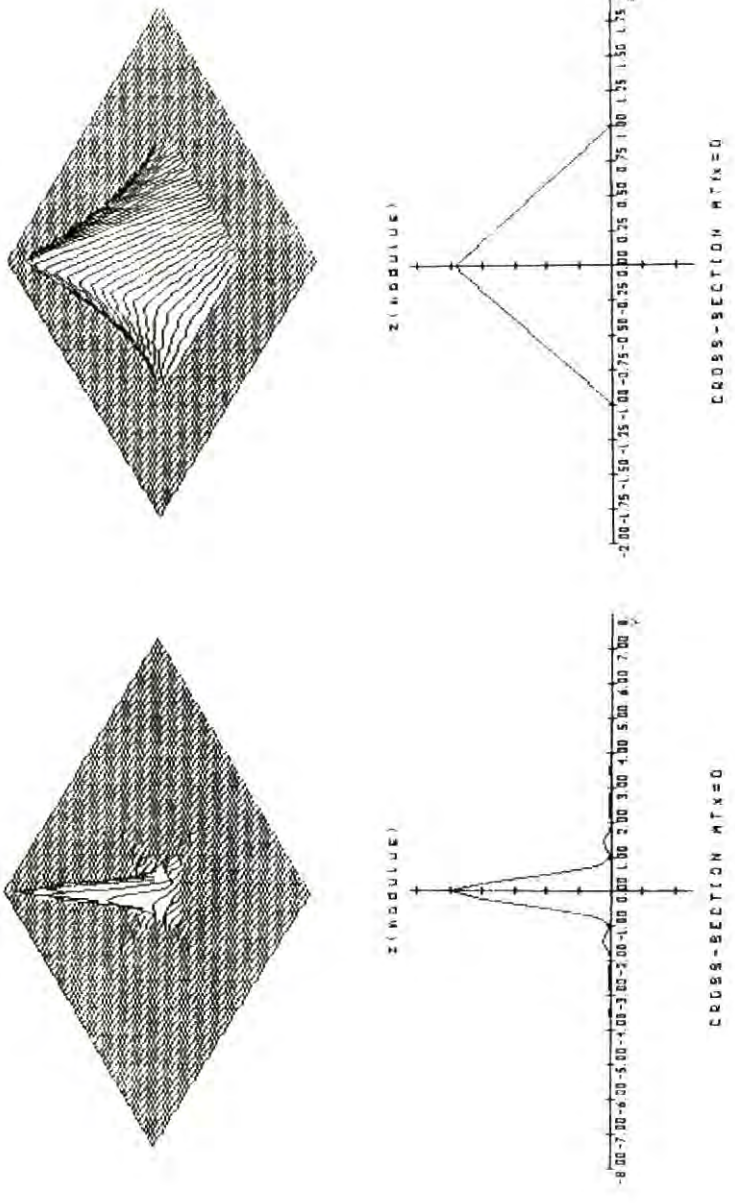

Figure 3. b) sinc^2, A = DxDy

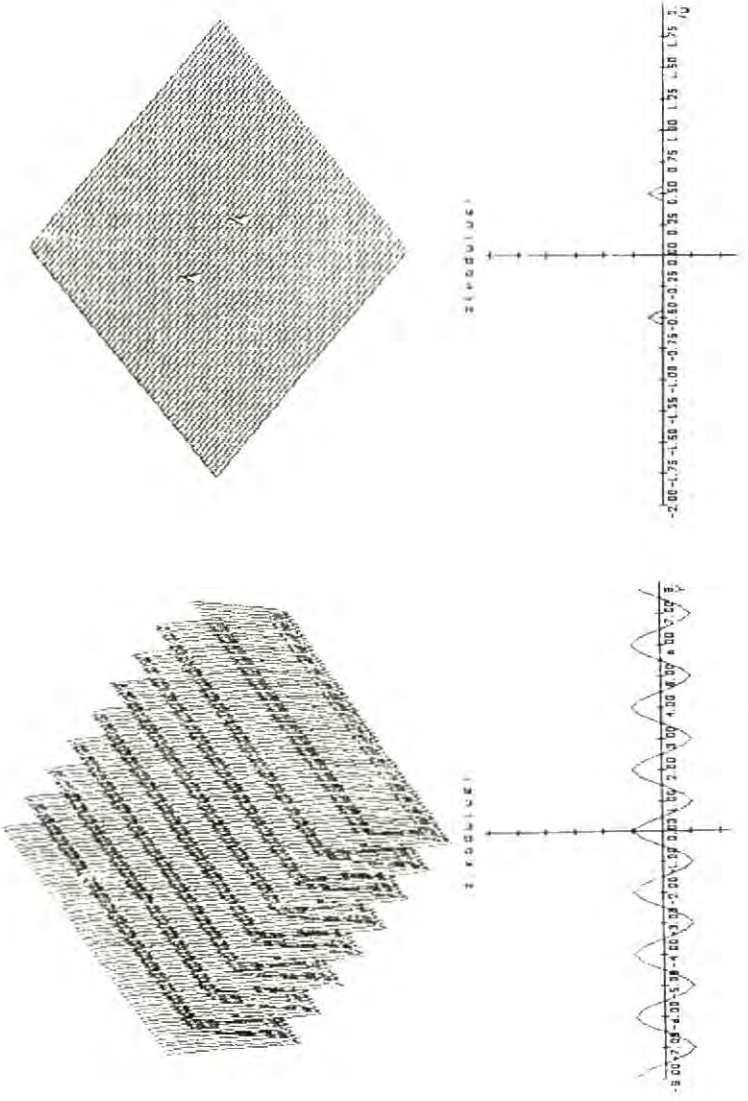

Figure 3. c) cos(y), A = 1/(NxNy)

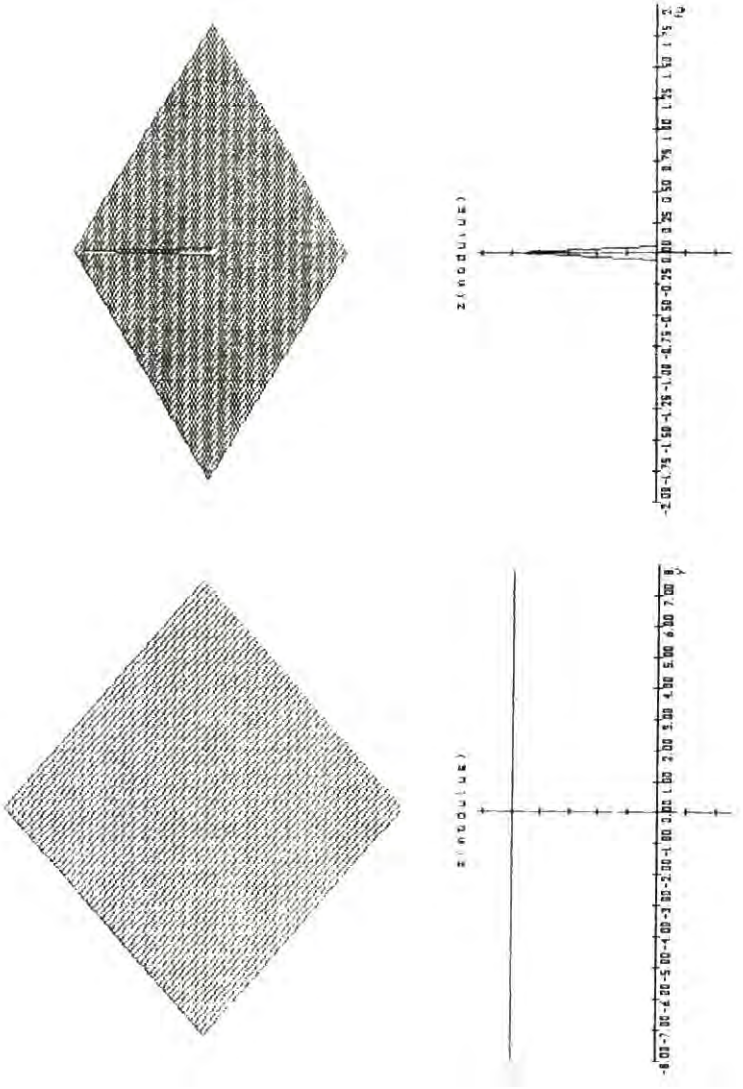

Figure 3. d) plane at z = 5, A = 1/(NxNy)

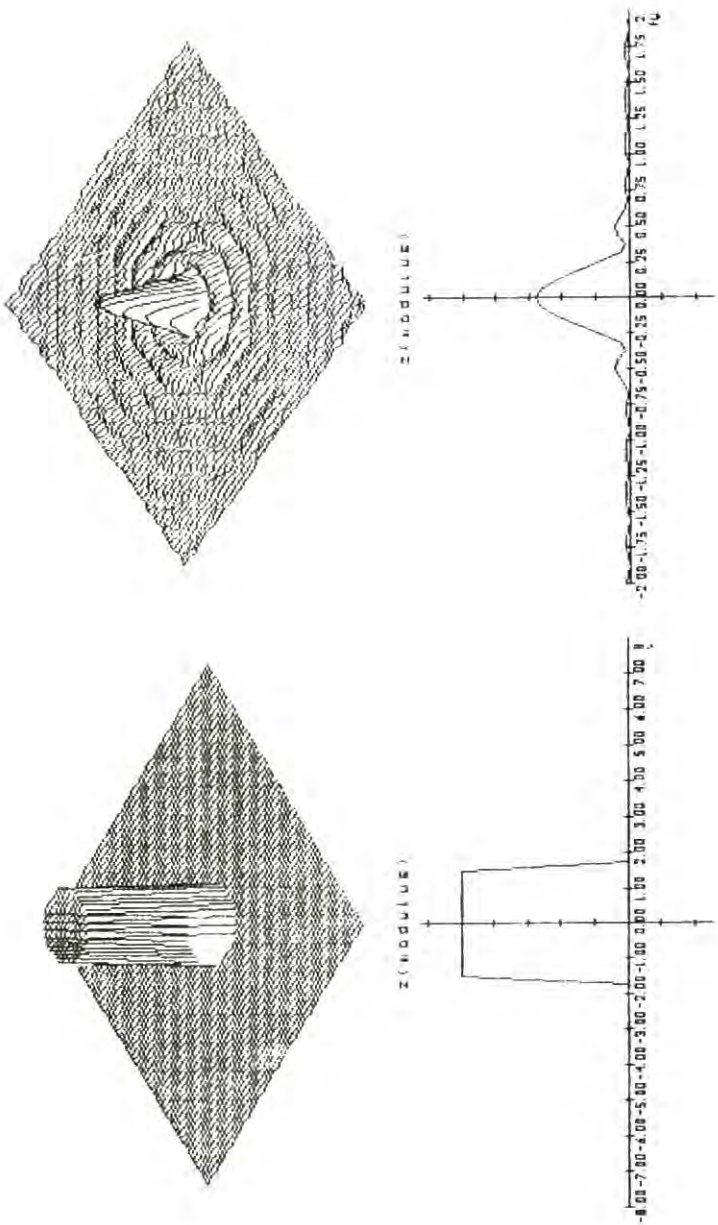

Figure 3. e) sombrero function, A = Dx/Nx

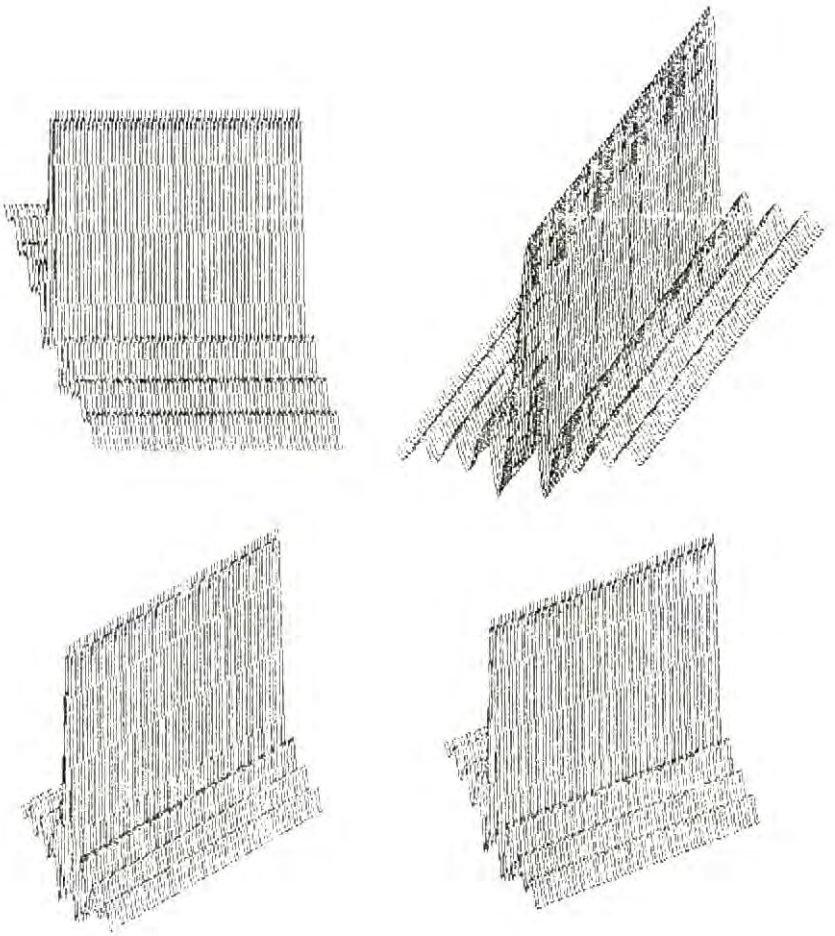

Figure 4. View of a one-dimensional sinc funtion from different perspectives: clockwise from top-left, $\alpha = 45$ deg, $\beta = 0$ deg; $\alpha = 0$ deg, $\beta = 45$ deg; $\alpha = 30$ deg, $\beta = 15$ deg; $\alpha = \beta = 20$ deg.

REFERENCES

Bracewell, R.N. The Fast Fourier Transform And Its Applications (McGraw-Hill, New York, 2nd Ed., 1986).

Brigham, E.O. The Fast Fourier Transform (Prentice-Hall, Inc., Engelwood Cliffs, 1974).

Cooley, J. and J. Tukey. "An algorithm for machine calculation of complex Fourier series," Math. Computation, 19, 297 (1965).

Gaskill, J.D. Linear Systems, Fourier Transforms, and Optics (John Wiley & Sons, New York, 1978) 454.

Gaylord, T. and E. Glytsis. Feature Editors, J. Opt. Soc. Am. A, August 1990 and September 1990, Special Issues on Grating Diffraction.

Press, W., B. Flannery, S. Teukolsky and W. Veterlling. Numerical Recipes: The Art of Scientific Computing (Cambridge University Press, Cambridge, 1988).

Rosenfeld, A. and A. Kac. Digital Picture Processing Volume 1 (Academic Press, New York, 1982, 2nd Ed.) Sections 6.3.3 and 7.2.

Rousseau, M. and J.P. Mathieu. Problems In Optics. (Pergamon Press, Oxford, 1973) 186.